Airborne Thermal Infrared Remote Sensing
Scott River Basin, CA

Submitted to:

Quartz Valley Indian Reservation
13601 Quartz Valley Road
Ft. Jones, CA 96032

Submitted by:

Watershed Sciences, Inc.
111 NW 2nd Street, Unit 1
Corvallis, OR 97330

Survey Date: August 10, 2006
Report Date: January 15, 2007
Revised Report: June 1, 2007

REPORT FOR THERMAL INFRARED REMOTE SENSING SCOTT RIVER BASIN, CA

Table of Contents

*Revised Report includes a Geo-Rectification section on page 7 and an updated list of deliverables

Background

In 2006, Quartz Valley Indian Tribe contracted with Watershed Sciences, Inc. to acquire airborne TIR and true color imagery of the Scott River and Shackleford Creek during the summer of 2006. The objective of the survey was to map surface water temperatures to support water quality and habitat assessments in the basin.

The TIR data were acquired between 15:00 and 16:57 PM on August 10, 2006. The flight was timed during mid-day to capture heat-of-the-day conditions. The map below (Figure 1) illustrates the extent of the airborne survey which covered the Scott River (57.0 miles) and Shackleford Creek from its mouth upstream to just past Back Meadows Creek (mile 8.9).

The flight on Shackleford Creek was intended to extend to the headwaters. However, several forest fires were active in the Klamath River basin during the time frame of the survey and temporary flight restrictions (TFRs) were in effect to the west of the Scott Valley. The Shackleford Creek TIR survey progressed toward an active fire area, which was controlled by a TFR. Due to the proximity to the TFR and the use of the valley corridors for fire fighting aircraft transiting to the Scott Valley Airport, the TIR survey of Shackleford Creek was ended at river mile 9.0 rather than the headwaters.

Watershed Sciences, Inc. deployed in-stream data loggers prior to the flight in order to calibrate and verify the accuracy of the TIR images. The sensors were deployed at regular spacing[1] (~10-miles) along the survey extent and were set to log kinetic temperatures at 10-minute intervals. The locations of the in-stream sensors are also illustrated in Figure 1.

Airborne TIR remote sensing has proven an effective method for mapping spatial temperature patterns in rivers and streams. These data are used to establish baseline conditions and direct future ground level monitoring. The TIR imagery illustrates the location and thermal influence of point sources, tributaries, and surface springs. This report details the work performed, including methodology and quantitative assessments of data quality. The images contained in this report are not meant to be comprehensive, but provide examples of image scenes and interpretations.

[1] As access permitted

Survey Extent

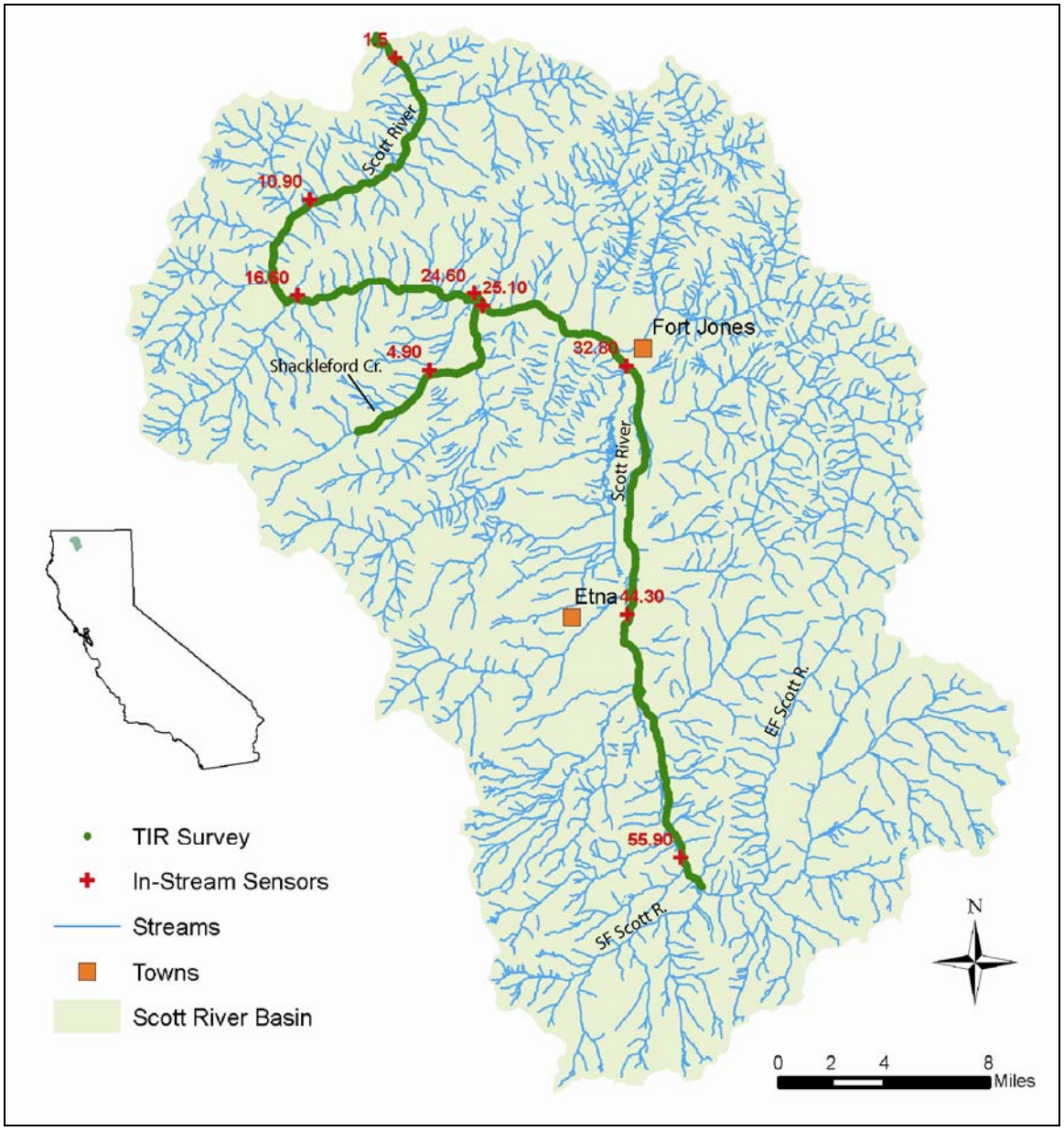

Figure 1 – The TIR survey was conducted along the Scott River from its confluence with the Klamath River upstream the confluence of the East and South Forks (57.0 miles). The survey included Shackleford Creek from its confluence with the Scott River upstream to river mile 8.9.

Methods

Data Collection

Instrumentation: Images were collected with a Space Instruments FireMapper 2.0 sensor (8-12μm) mounted on the underside of a Bell Jet Ranger Helicopter (Figure 2). The TIR sensor was co-mounted with a high-resolution true color digital camera (*Nikon D2X w/ 24mm lens, 6.9 mega-pixels*). Both cameras were positioned to look vertically down from the aircraft (nadir). The Firemapper 2.0 is a calibrated radiometer with internal non-uniformity correction and drift compensation. General specifications of the thermal infrared sensor are listed in Table 1.

Thermal infrared images were recorded directly from the sensor to an on-board computer as raw counts, which were than converted to radiant temperatures. The individual images were referenced with time, position, and heading information provided by a global positioning system (GPS).

Figure 2 – Bell Jet Ranger equipped with a thermal infrared radiometer and high resolution digital camera. The sensors are contained in a composite fiber enclosure attached to the underside of the helicopter and flown longitudinally along the stream channel.

Table 1. Summary of TIR sensor specifications.

Sensor:	Space Instruments Firemapper 2.0
Wavelength:	8-12μm
Temperature Resolution:	0.01°C
Noise Equivalent Temperature Differences (NETD)	0.07°C
Pixel Array	320 (H) x 240 (V)
Encoding Level:	16 bit
Horizontal Field-of-View:	44.3°

Image Characteristics: The aircraft was flown longitudinally along the stream corridor in order to have the river in the center of the display. The objective was for the stream to occupy 30-60% of the image. The TIR sensor is set to acquire images at its maximum rate (*~1 image/2 seconds*) resulting in considerable vertical overlap between images.

Ground Control: Watershed Sciences deployed in-stream data loggers prior to the flight in order to calibrate and verify the accuracy of the TIR data. The data loggers were distributed at public access points along the survey extent. The sensors were placed on the bottom of the river in locations with good vertical mixing. Watershed Sciences sensors were deployed to support the flight and were only in the stream during the day of the survey.

Data Processing

Calibration: Prior to the season, the response characteristics of the sensor are measured in a laboratory environment. The response curves relate the raw digital numbers recorded by the sensor to emitted radiance from the black body. The raw TIR images collected during the survey initially contain raw digital numbers which are then converted to radiance values (*W/m^2*sr*micron*) based on the pre-season calibration.

The radiance values were adjusted based on a comparison of the measured radiance to the calculated radiance at each ground truth location. This adjustment was performed to correct for path length attenuation and the emissivity of natural water. The in-stream data were assessed at the time the image was acquired, with radiant values representing the median of ten points sampled from the image at the data logger location. The radiance values were then converted to surface temperatures using Planck's Black Body equation.

Interpretation and Sampling: Once calibrated, the images were integrated into a GIS in which an analyst interpreted and sampled stream temperatures. Sampling consisted of querying radiant temperatures (pixel values) from the center of the stream channel and saving the median value of a ten-point sample to a GIS database file. The temperatures of detectable surface inflows (i.e. surface springs, tributaries) were also sampled at their mouths. During sampling, the analyst provided interpretations of the spatial variations in surface temperatures observed in the images.

Geo-referencing: The images are tagged with a GPS position and heading at the time they are acquired. Since the TIR camera is maintained at vertical down-look angles, the geographic coordinates provide a reasonably accurate index to the location of the image scene. Due to the relatively small footprint of the imagery and independently stabilized mount, image pixels are not individually registered to real world coordinates. The image index is saved as an ESRI point shapefile containing the image name registered to an X and Y position (UTM Zone 10, NAD83) of sensor location at time of capture. In order to provide further spatial reference, the TIR images were assigned a river mile based on a routed stream layer (Figure 3).

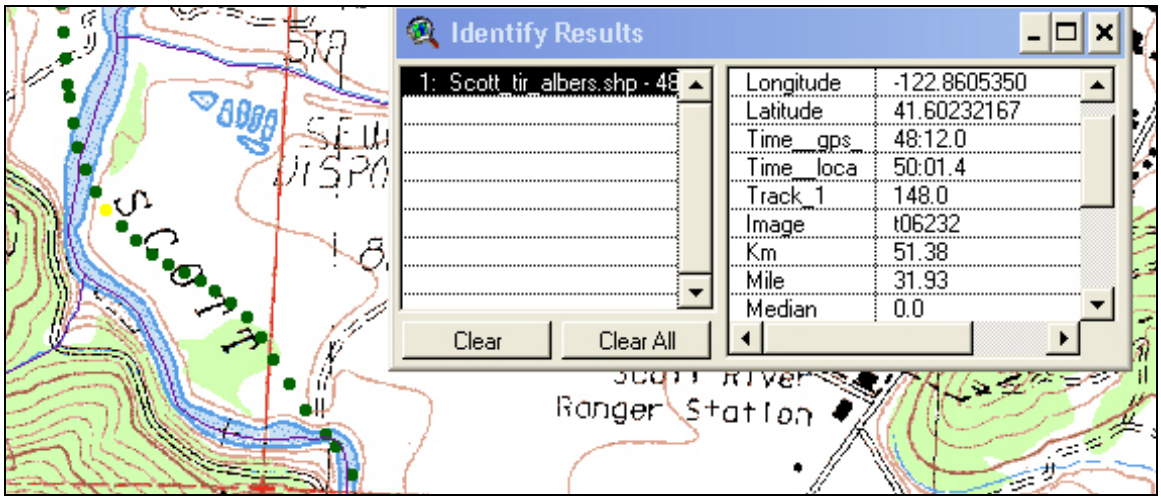

Figure 3 –Each point on the map represents a thermal image location. The inset box shows the information recorded with each image point during acquisition.

Geo-Rectification: The TIR images were geo-rectified to real world coordinates using the National Agriculture Imagery Program's (NAIP) ortho-photos as a reference layer. The TIR images were initially oriented using the position and directional information collected on the aircraft. Individual frames were then geo-rectified by finding a minimum of six common ground control points (GCP's) between the TIR images and existing NAIP ortho-photos (average of 12). The images were then warped using a 1^{rst} order polynomial transformation. The geo-rectification does not incorporate a digital elevation model for correcting terrain displacement. However, due to the small ground footprint of the frame and the relatively flat valley floor, these spatial distortions are considered minimal.

Temperature Profiles: The median temperatures for each sampled image were plotted versus the corresponding river mile to develop a longitudinal temperature profile. The profile illustrates how stream temperatures vary spatially along the stream gradient. The location and median temperature of all sampled surface water inflows (e.g. tributaries, surface springs, etc.) are included on the plot to illustrate how these inflows influence the main stem temperature patterns. Radiant temperatures were only sampled along what appeared to be the main flow channel in the river.

Thermal Image Characteristics

Surface Temperatures: Thermal infrared sensors measure TIR energy emitted at the water's surface. Since water is essentially opaque to TIR wavelengths, the sensor is only measuring water surface temperature. Thermal infrared data accurately represents bulk water temperatures where the water column is thoroughly mixed; however, thermal stratification can form in reaches that have little or no mixing. Thermal stratification in a free flowing river is inherently unstable due to variations in channel shape, bed composition, and in-stream objects (i.e. rocks, trees, debris, etc.) that cause turbulent flow and can usually be detected in the imagery.

Expected Accuracy: Thermal infrared radiation received at the sensor is a combination of energy emitted from the water's surface, reflected from the water's surface, and absorbed and re-radiated by the intervening atmosphere. Water is a good emitter of TIR radiation and has relatively low reflectivity (~ 4 to 6%). However, variable water surface conditions (i.e. riffle versus pool), slight changes in viewing aspect, and variable background temperatures (i.e. sky versus trees) can result in differences in the calculated radiant temperatures within the same image or between consecutive images. The apparent temperature variability is generally less than 0.5^{o}C (Torgersen et al. 2001[2]). However, the occurrence of reflections as an artifact (or noise) in the TIR images is a consideration during image interpretation and analysis. In general, apparent stream temperature changes of < 0.5^{o}C are not considered significant unless associated with a surface inflow (e.g. tributary).

Differential Heating: In stream segments with flat surface conditions (i.e. pools) and relatively low mixing rates, observed variations in spatial temperature patterns can be the result of differences in the instantaneous heating rate at the water's surface. In the TIR images, indicators of differential surface heating include seemingly cooler radiant temperatures in shaded areas compared to surfaces exposed to direct sunlight.

Feature Size and Resolution: A small stream width logically translates to fewer pixels "in" the stream and greater integration with non-water features such as rocks and vegetation. Consequently, a narrow channel (relative to the pixel size) can result in higher inaccuracies in the measured radiant temperatures. This is a consideration when sampling the radiant temperatures at tributary mouths and surface springs.

Temperatures and Color Maps: The TIR images collected during this survey consist of a single band. As a result, visual representation of the imagery *(in a report or GIS environment*) requires the application of a color map or legend to the pixel values. The selection of a color map should highlight features most relevant to the analysis (i.e. *spatial variability of stream temperatures*). For example, a continuous, gradient style

[2] Torgersen, C.E., R. Faux, B.A. McIntosh, N. Poage, and D.J. Norton. 2001. Airborne thermal remote sensing for water temperature assessment in rivers and streams. *Remote Sensing of Environment* 76(3): 386-398.

color map that incorporates all temperatures in the image frame will provide a smoother transition in colors throughout the entire image, but will not highlight temperature differences in the stream. Conversely, a color map that focuses too narrowly cannot be applied to the entire river and will "washout" terrestrial and vegetation features.

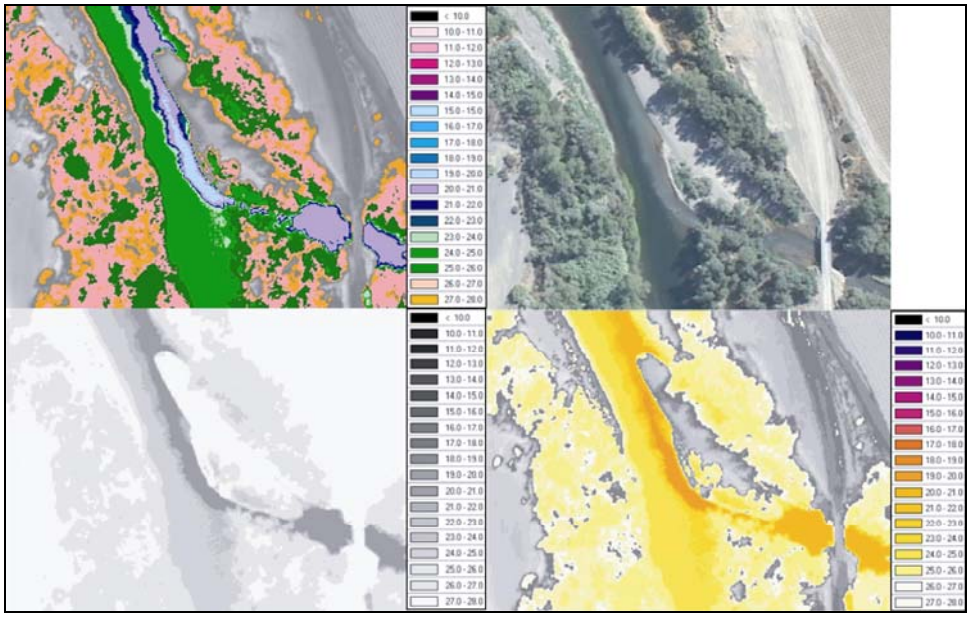

Figure 4 - Example of different color maps applied to the same TIR image.

Image Uniformity: The TIR sensor used for this study uses a focal plane array of detectors to sample incoming radiation. A challenge when using this technology is to achieve uniformity across the detector array. This sensor has an automatic correction scheme which nearly eliminates non-uniformity across the image frame.

Acquisition Parameters

Table 2. TIR Image Acquisition Parameters for the Scott River and Shackleford Creek.

Date:	August 9, 2006
Time:	14:24 – 15:59
Flight Above Ground Level (AGL):	305 m (1000 ft)
Image Footprint Width:	251 m (822 ft)
Native Pixel Resolution:	0.7 m (2.57 ft)

Weather Conditions

The weather conditions for the flight were considered good with mostly clear skies and warm temperatures (Table, 3; Figure 5). However, smoke from fire complexes to the West of the Scott River Valley reduced visibility through portions of the survey extent. There was very little visible smoke downstream of Fort Jones. The level of smoke increased moving upstream through the valley. While the thermal IR sensor "sees" through the smoke and radiant temperature measurements are not effected, the smoke reduces light levels and path transmittance in the true color imagery resulting in a "hazier" image.

Table 3 – Hourly weather conditions observed at the Scott Valley Airport, CA 8/10/06.

Time PDT	Temp °F	Temp °C	Dew Point	Humidity %	Wind Direction	Wind Speed (MPH)	Conditions
12:53 PM	84.9	29.4	46.9	27	Variable	5.8	Clear
1:53 PM	86.0	30.0	45.0	24	Calm	Calm	Clear
2:53 PM	87.1	30.6	46.0	24	NNW	10.4	Scattered Clouds
3:53 PM	87.1	30.6	48.0	26	North	11.5	Partly Cloudy
4:53 PM	86.0	30.0	51.1	30	NNE	17.3	Partly Cloudy
5:53 PM	84.0	28.9	50.0	31	NNE	18.4	Partly Cloudy

Figure 5 – Ground level digital photo of the Scott River on the morning of August 10, 2006. Conditions were ideal through most of the survey extent. However, smoke from nearby wildfires was a factor on the upper reaches of the Scott River during the time frame of the survey.

Thermal Accuracy

Table 4 provides a comparison between the kinetic temperatures recorded by the in-stream data loggers and the radiant temperatures derived from the TIR images. The range of differences was well within the radiant temperature accuracies observed during other TIR surveys in Western States over the past eight years. However, since the in-stream data were used to compute an adjustment to the radiant temperatures, they should not be considered an independent check of radiant temperatures. The correction was computed as an average offset from the raw radiant values for all sensor locations.

Table 4 – Comparison of radiant temperatures derived from the TIR images and kinetic temperatures from the in-stream monitors.

Stream	SN	Pass	Image	Local	mile	Kinetic °C	Radiant °C	Difference °C
Scott River								
Scott	540664	2	ir1-0052	15:03	1.5	23.0	23.0	0.00
Scott	540663	3	ir1-0284	15:17	10.9	21.4	21.3	0.10
Scott	1026262	4	ir1-0210	15:26	16.6	22.7	22.6	0.10
Scott	766181	5	ir1-0279	15:39	24.6	23.8	23.6	0.20
Scott	882337	6	ir1-0259	15:51	32.8	25.4	25.3	0.07
Scott	1026260	7	ir1-0402	16:05	44.3	22.3	22.3	0.00
Scott	882338	8	ir1-0461	16:22	55.9	22.7	22.4	0.30
Shackleford Creek								
Scott	766181	9	ir1-0037	16:40	0.0	23.8	23.7	0.1
Shackleford Cr.	766182	9	ir1-0220	16:46	4.9	16.3	16.5	-0.2

Results

Scott River

Longitudinal Temperature Profile

Median channel temperatures were plotted versus river mile for the Scott River from its mouth upstream to the confluence of the South and East Forks (Figure 6). Tributaries sampled during the analysis are labeled on the profile by river mile and listed in Table 5. Seeps and side-channels were also sampled during the analysis. The locations of these features were included on the longitudinal profile to provide additional context for interpreting spatial temperature patterns and are listed in Table 6. Side channels were identified as surface water that originates within the main channel and reconnects further downstream. In general, the analyst only sampled side channels that differed in surface temperature from the main flow. Springs/seeps were identified as discharge into the main channel that appeared to originate as sub-surface upwelling. Landmarks such as towns and bridges are shown to provide additional context for interpretation of the profile.

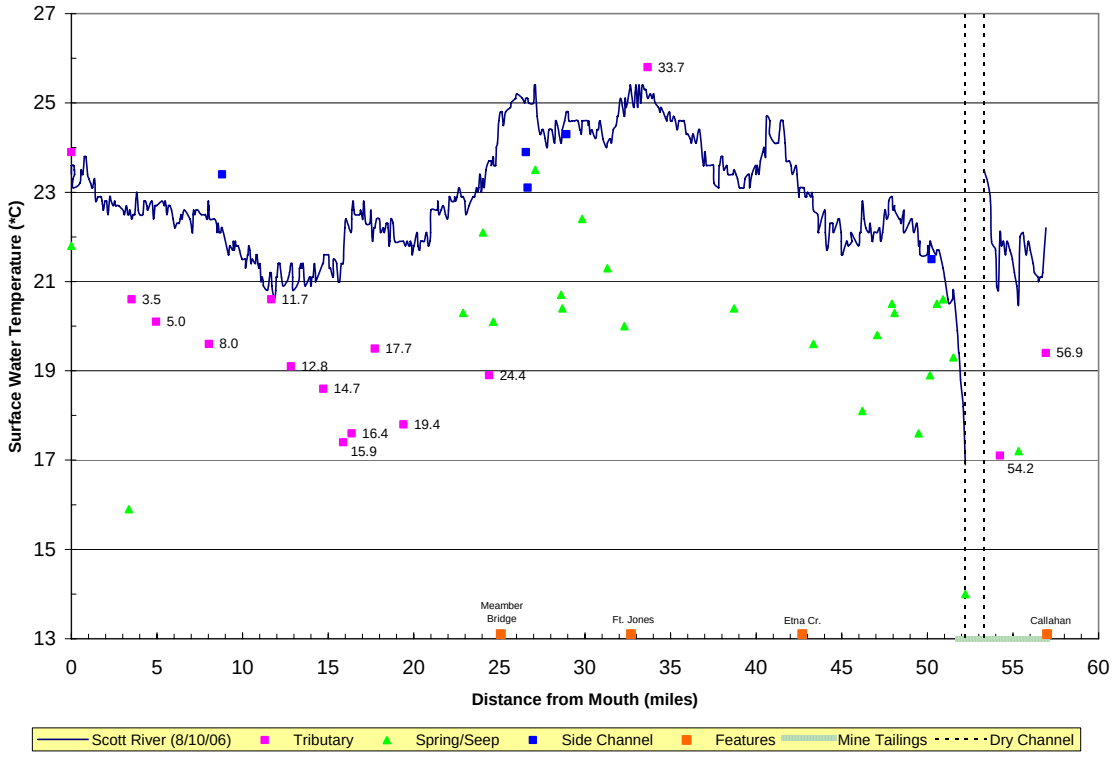

Figure 6 - Median channel temperatures plotted versus river mile for the Scott River. The locations of detected surface inflows are illustrated on the profile and labeled by river mile.

Table 5 - Tributaries sampled along the Scott River.

Tributary	Image	km	mile	Tributary °C	Scott R. °C	Difference °C
Klamath R.	t02005	0.00	0.00	23.9	23.4	0.5
Mill Cr. (RB)	t03064	5.67	3.52	20.6	22.4	-1.8
Pat Ford Cr. (RB)	t03103	7.96	4.95	20.1	22.7	-2.6
Schuler Cr (RB)	t03189	12.94	8.04	19.6	22.7	-3.1
Tomkins Cr. (LB)	t04046	18.80	11.68	20.6	21.2	-0.6
Middle Cr. (LB)	t04084	20.63	12.82	19.1	21.4	-2.3
Kelsey Cr. (LB)	t04146	23.68	14.72	18.6	21.4	-2.8
Canyon Cr. (LB)	t04187	25.55	15.87	17.4	21.4	-4.0
Boulder Cr. (LB)	t04198	26.34	16.37	17.6	22.4	-4.8
Unnamed Tributary (LB)	t05056	28.54	17.73	19.5	22.2	-2.7
Isinglass Cr. (LB)	t05109	31.22	19.40	17.8	21.9	-4.1
Shackeford Cr (Seep) (LB)	t05273	39.27	24.40	18.9	23.7	-4.8
Unnamed Tributary (RB)	t07041	54.16	33.66	25.8	25.1	0.7
Sugar Cr (LB)	t08371	87.30	54.24	17.1	22.1	-5.0
SF Scott R (LB)	t08452	91.61	56.93	19.4	22.2	-2.8

Table 6 - Springs, seeps, and side channels sampled along the Scott River.

Tributary	Image	km	mile	Tributary °C	Median °C	Difference °C
Spring/Seep						
Seep (RB)	t02009	0.00	0.00	21.8	23.6	-1.8
Spring (LB)	t03059	5.41	3.36	15.9	22.5	-6.6
Seep (RB)	t05227	36.82	22.88	20.3	22.9	-2.6
Seep (RB)	t05262	38.69	24.04	22.1	23.3	-1.2
Seep (LB)	t05283	39.66	24.64	20.1	23.8	-3.7
Seep (LB)	t06086	43.61	27.10	23.5	25.4	-1.9
Seep (LB)	t06132	46.04	28.61	20.7	24.1	-3.4
Seep (RB)	t06136	46.16	28.68	20.4	24.4	-4.0
Seep (LB)	t06171	48.03	29.84	22.4	24.6	-2.2
Seep (RB)	t06212	50.39	31.31	21.3	24.1	-2.8
Seep (LB)	t06243	51.98	32.30	20.0	24.7	-4.7
Seep (RB)	t07218	62.30	38.71	20.4	23.5	-3.1
Seep (LB)	t07369	69.76	43.35	19.6	22.6	-3.0
Seep (LB)	t08077	74.37	46.21	18.1	22.8	-4.7
Seep (RB)	t08107	75.75	47.07	19.8	22.1	-2.3
Seep (LB)	t08174	77.13	47.93	20.5	22.9	-2.4
Seep (RB)	t08181	77.38	48.08	20.3	22.7	-2.4
Spring (RB)	t08223	79.65	49.49	17.6	21.8	-4.2
Spring (RB)	t08242	80.71	50.15	18.9	21.9	-3.0
Seep (LB)	t08258	81.36	50.55	20.5	21.7	-1.2
Seep (RB)	t08266	81.95	50.92	20.6	21.3	-0.7
Spring (LB)	t08287	82.91	51.52	19.3	20.8	-1.5
Spring (LB)	t08308	84.05	52.22	14.0	16.9	-2.9
Spring (RB)	t08408	89.05	55.33	17.2	20.5	-3.3
Side Channel						
Side Channel (LB)	t03215	14.18	8.81	23.4	22.2	1.2
Side Channel (RB)	t06067	42.73	26.55	23.9	25.1	-1.2
Side Channel (LB)	t06071	42.89	26.65	23.1	25.1	-2.0
Side Channel (LB)	t06145	46.53	28.91	24.3	24.8	-0.5
Side Channel (LB)	t08246	80.88	50.25	21.5	21.8	-0.3

Observations and Analysis

Inspection of the longitudinal temperature profile (Figures 6) illustrates distinct patterns of warming and cooling at different spatial scales. A total of 14 tributaries and 24 springs/seeps were sample during the analysis of the imagery. These discharges (both individually and collectively) influenced the bulk temperatures in the Scott River. The following paragraphs examine the spatial temperature patterns and offer some hypotheses on the physical processes driving the observed trends. In some cases, sample images (*next section of this report*) are provided to help illustrate thermal features or channel conditions.

At their confluence, the South Fork Scott River (19.4^{o}C) had surface water temperatures that were ~2.8^{o}C cooler than the East Fork (22.2^{o}C) *(Image Scott1*). Radiant temperatures were ~21.1^{o}C downstream of the mixing zone with some local variability observed between mile 56.7 and 53.3. A spring (mile 55.3) and Sugar Creek (mile 54.2) both discharged cooler water to the Scott River and contributed to the spatial temperature variability observed within this reach (*Images Scott2 & Scott3*). At mile 53.3, the Scott River went sub-surface with very little water visible in the river channel. The channel was mostly dry to river mile 52.2 where the river re-emerged with considerably cooler water temperatures (16.9^{o}C) (*Image Scott4*). The dry channel and sub-sequent upwelling of flow in the channel resulted in a dramatic decrease in temperatures that is evident the longitudinal temperature profile. Mine tailings bordered the river within this reach (i.e. the town of Callahan to mile 52.2) and the substrate constitution of these tailings may have contributed to some of the spatial temperature variability observed in this reach.

Once the Scott River re-emerged at mile 52.2, radiant stream temperatures increased rapidly downstream reaching 21.7^{o}C by river mile 50.7. Between mile 50.7 and 43.6, radiant water temperatures exhibited local spatial variability, but no consistent pattern of warming or cooling. Surface temperatures reached a local maximum of 22.9^{o}C at mile 47.9 and a local minimum of 21.6^{o}C at mile 45.1. The detection of a number of seeps (9) indicates the presence of some level of hyporheic flow within this reach. These shallow sub-surface exchanges often buffer heating processes and may be the reason that the stream did not warm significantly in this reach (*Image Scott5*). These exchanges may also contribute to the local spatial variability observed in the profile with localized cooling occurring in areas of sub-surface discharge and more rapid heating in areas where surface flow is lost.

Moving downstream, radiant water temperatures increased from ~22.1^{o}C at mile 43.6 to a survey maximum of 25.3^{o}C at mile 33.6. There were two seeps/springs detected within this reach. The fewer number of seeps and the increase in longitudinal heating suggests an absence (or at least decrease) in the processes buffering heating in the upstream reach. A prominent pattern within this reach was a rapid increase in temperature near mile 41.6 (24.6^{o}C) followed by a rapid decrease in surface temperatures at mile 40.6 (*Image Scott6)*. The magnitude of radiant temperature change was well outside noise levels typically associated with airborne TIR remote sensing (i.e. ±0.5^{o}C). The spatial

temperature pattern suggests that surface water is lost from the main channel near mile 41.6 resulting in increased longitudinal heating. This heating is subsequently followed by a decrease in stream temperatures as sub-surface flow re-enters the channel. A rapid response in bulk water temperatures, such as observed at this location, is normally observed under very low flow conditions.

Radiant water temperatures remained relatively warm between river miles 33.5 (25.3°C) and 25.4 (24.8°C). This reach extended from just upstream of Ft. Jones downstream to the Meamber Bridge. Six springs/seeps were detected within this reach and sub-surface flow probably contributed to the observed 1.4°C decrease in water temperatures between river miles 32.6 and 24.1. Moving downstream, a sharp 1.0°C increase in apparent water temperature was observed at river mile 27.1. The reason for this rapid increase in temperatures could not be determined directly from the imagery. However, as mentioned previously, rapid increases in longitudinal heating are typically associated with changes in the physical processes that govern stream heating such as a loss of in-stream flow, a decrease in hyporheic flow, or change in the level of riparian shading.

Between river miles 25.5 and 19.9, radiant water temperatures in the Scott River decreased from 24.8°C to 21.6°C, a drop of 3.2°C. Shackelford Creek (mile 24.4) was detected in this reach, but had very little surface flow. Four seeps/springs were sampled within this reach including one at the mouth of Shackleford Creek, but appeared to have only a local influence on bulk water temperatures. Inspection of the longitudinal temperature profile in relation to 1:24K topographic base maps shows that the downstream cooling trend begins at the lower end of the Scott Valley and continues into the canyon. In this case, the Scott River transitions from the broad Scott Valley to the narrower canyon reach. The constriction of the valley often results in sub-surface flow being forced back into channel and subsequent cooling of stream temperatures. Past TIR surveys have shown that transitions in geomorphology and valley form are almost always inflection points in the longitudinal temperature profiles.

Proceeding downstream, water temperatures showed a slight increase between river mile 19.9 (21.6°C) and 16.5 (22.8°C) before exhibiting a continued decrease reaching a local minimum at river mile 11.7. In contrast to the Scott Valley, ten tributaries were sampled through the canyon reach and each contributed cooler water to the main stem. The inflows of Boulder Creek (mile 16.4) and Canyon Creek (mile 15.9) decreased bulk temperatures in the Scott River by ~1.8°C (*Image Scott 8*). From river mile 11.7, stream temperatures in the Scott River increased steadily reaching 23.6°C at its confluence with the Klamath River.

Sample Images

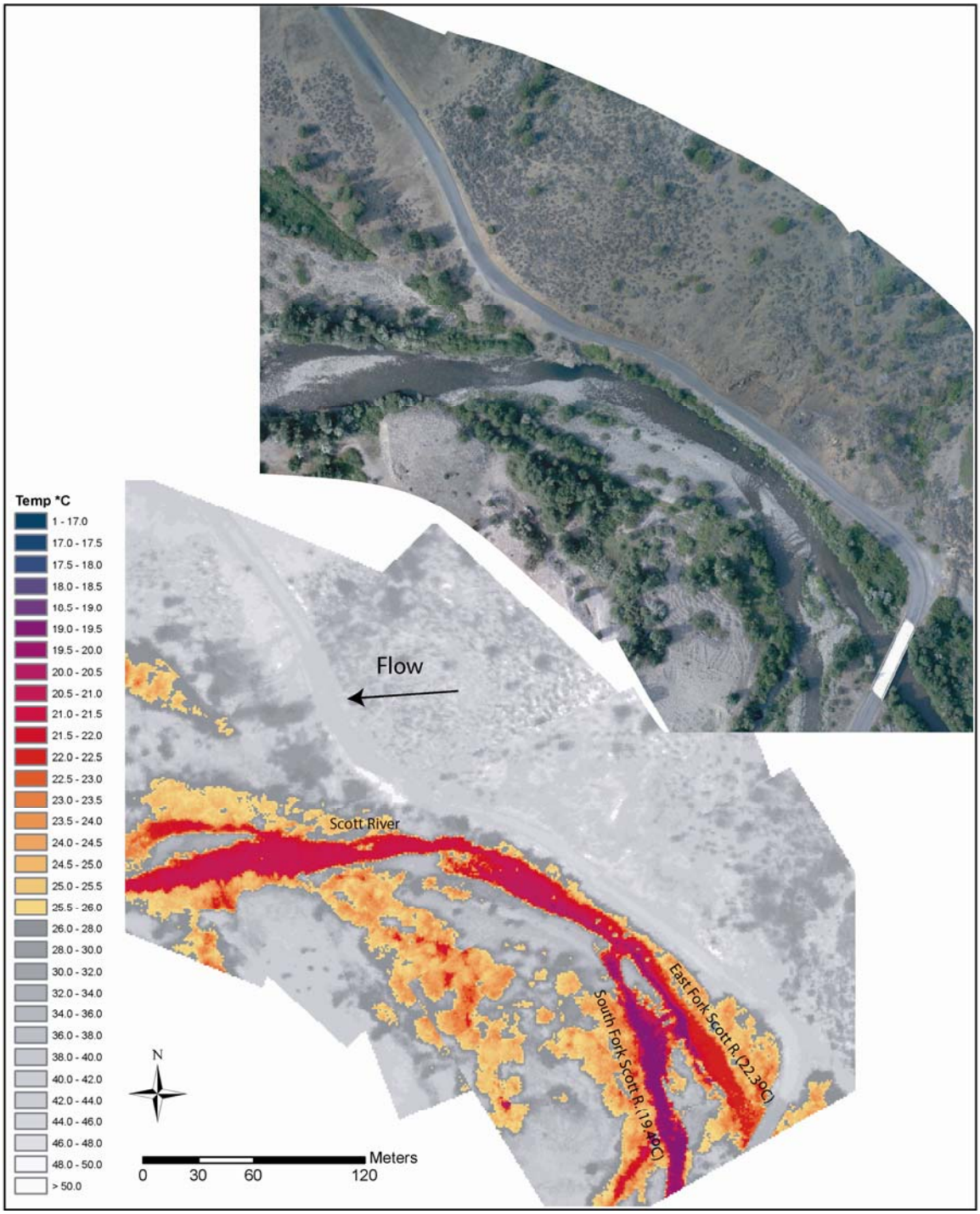

Scott 1 – TIR (bottom) and true color (top) image showing the confluence of the South (19.4°C) and East Fork (22.2°) of the Scott River. (*TIR frames: 8446_8452*).

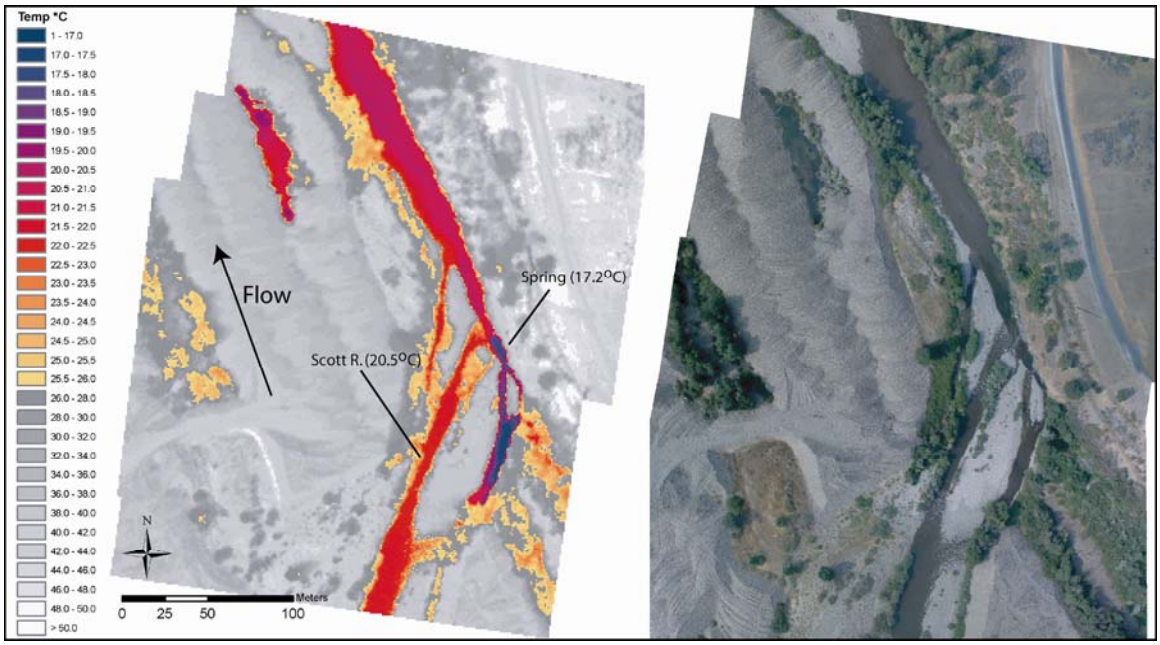

Scott 2 – The TIR (left) and true color (right) image above show a spring (17.2 °C) at mile 55.2. The discharge from the spring and from Sugar Creek at mile 54.3 contributed to the spatial thermal variability observed within this reach *(TIR frames: 8407_8410).*

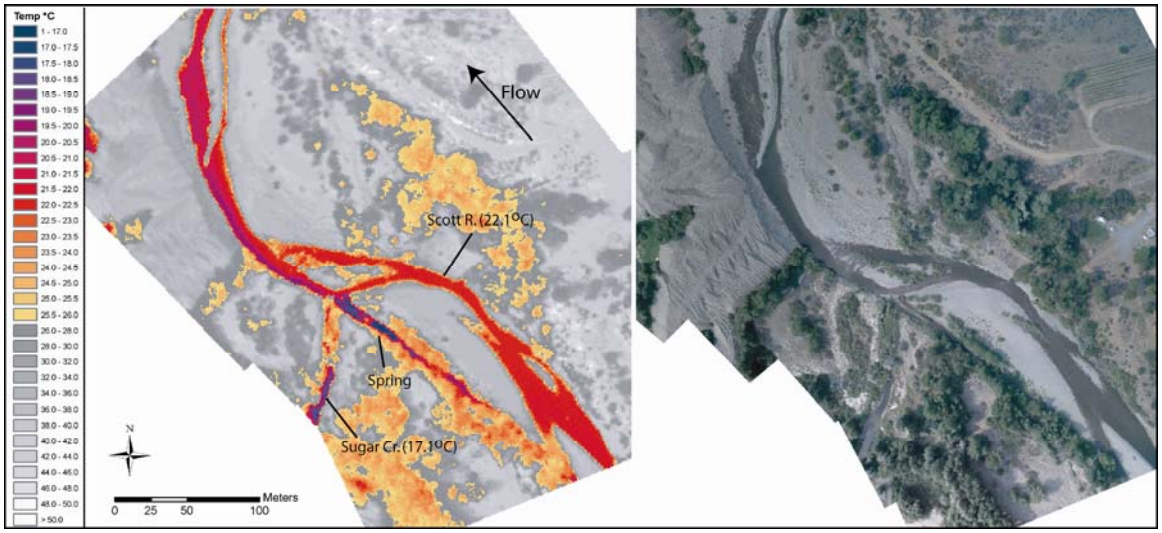

Scott 3 – The TIR (left) and true color (right) image show the inflow of Sugar Creek (17.1°C) at mile 54.3 in the Scott River. An apparent spring appears just upstream of the mouth of Sugar Creek. *(TIR frames: 8368_8374 Sugar Creek)*

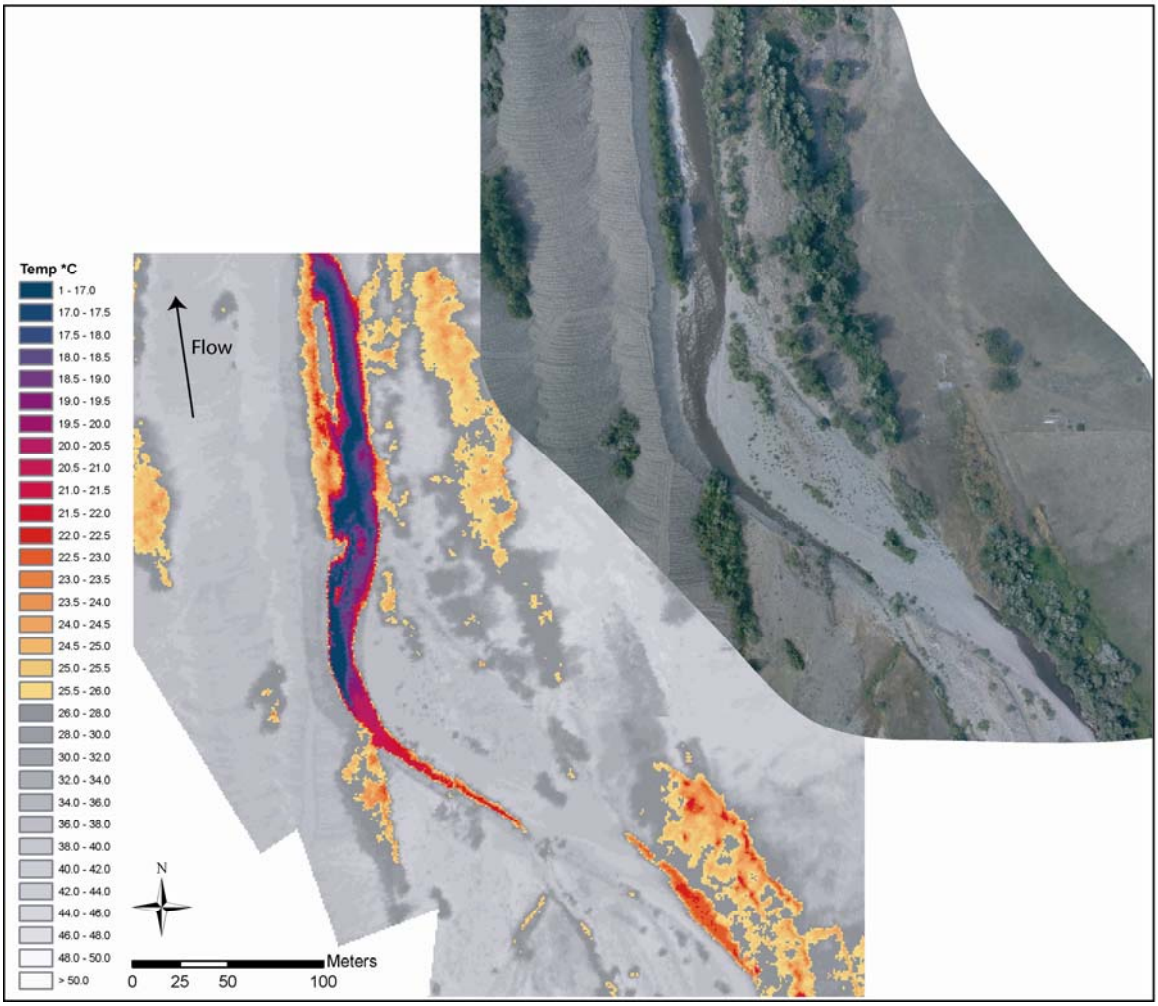

Scott 4 – The TIR (bottom) and true color (top) image show the Scott River at mile 52.2 where the Scott River re-emerges from the channel substrate. The channel was mostly dry between this location and mile 53.3. (*TIR frames: 8304_8313*).

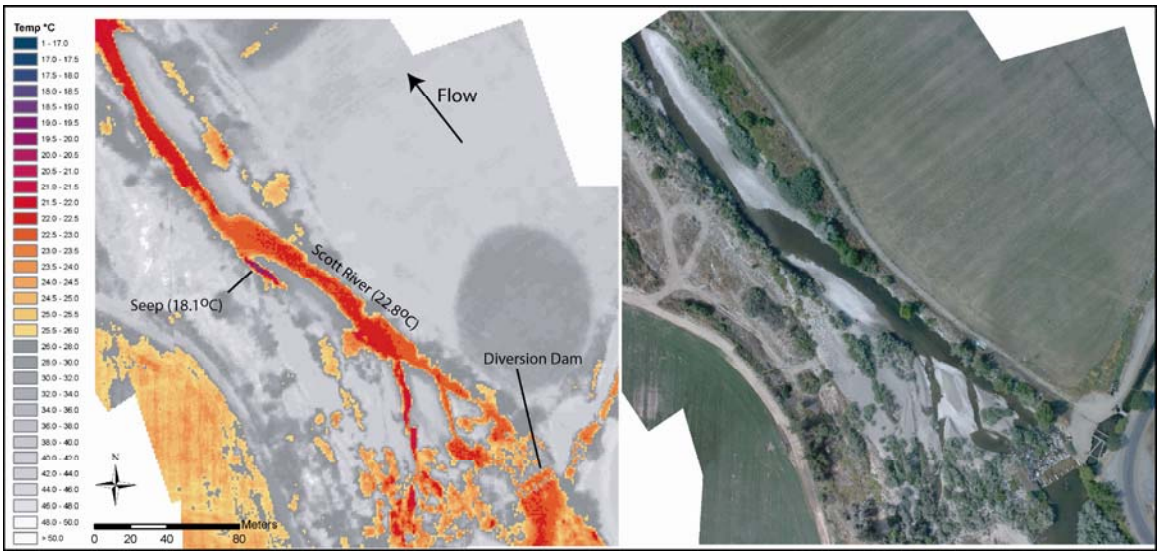

Scott 5 – The TIR (left) and true color (right) image show a spring/seep in the Scott River at mile 46.2. A total of nine seeps/springs were sampled in this reach and are evidence of hyporheic flow. The shallow sub-surface exchanges in this reach likely contributed to both the lack of downstream warming and the local spatial variability observed in this reach. (*TIR frames: 8075_8080*)

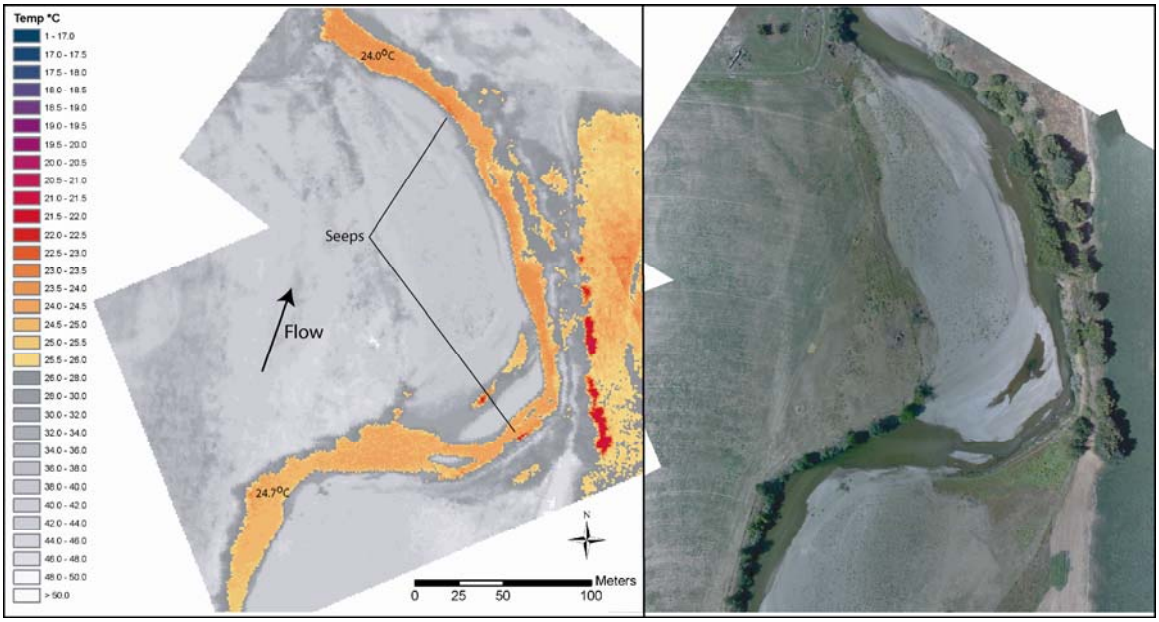

Scott 6 – The TIR (left) and true color (right) images show the location of a rapid drop in surface temperature in the Scott River at mile 40.6. The apparent seeps along both banks of the river and the magnitude of the decrease suggest sub-surface influence on bulk water temperatures at this location (*TIR Frames: 7276_7283*).

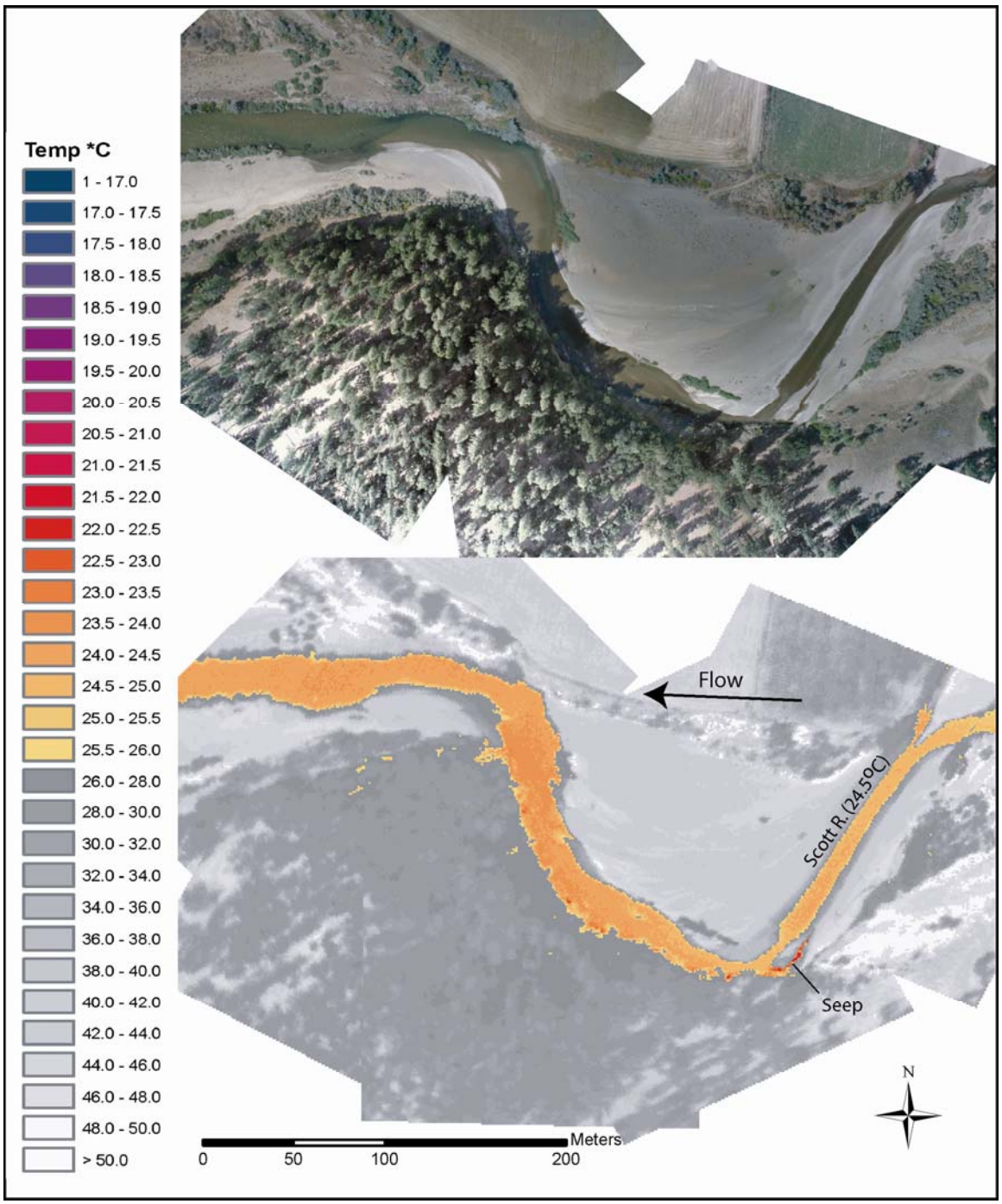

Scott 7 – The TIR (bottom) and true color (top) image showing a small seep along the left bank of the Scott River at mile 29.8. The image is representative of the general channel conditions at between river miles 32.6 and 25.5. (*TIR Frames: 6168_6173*).

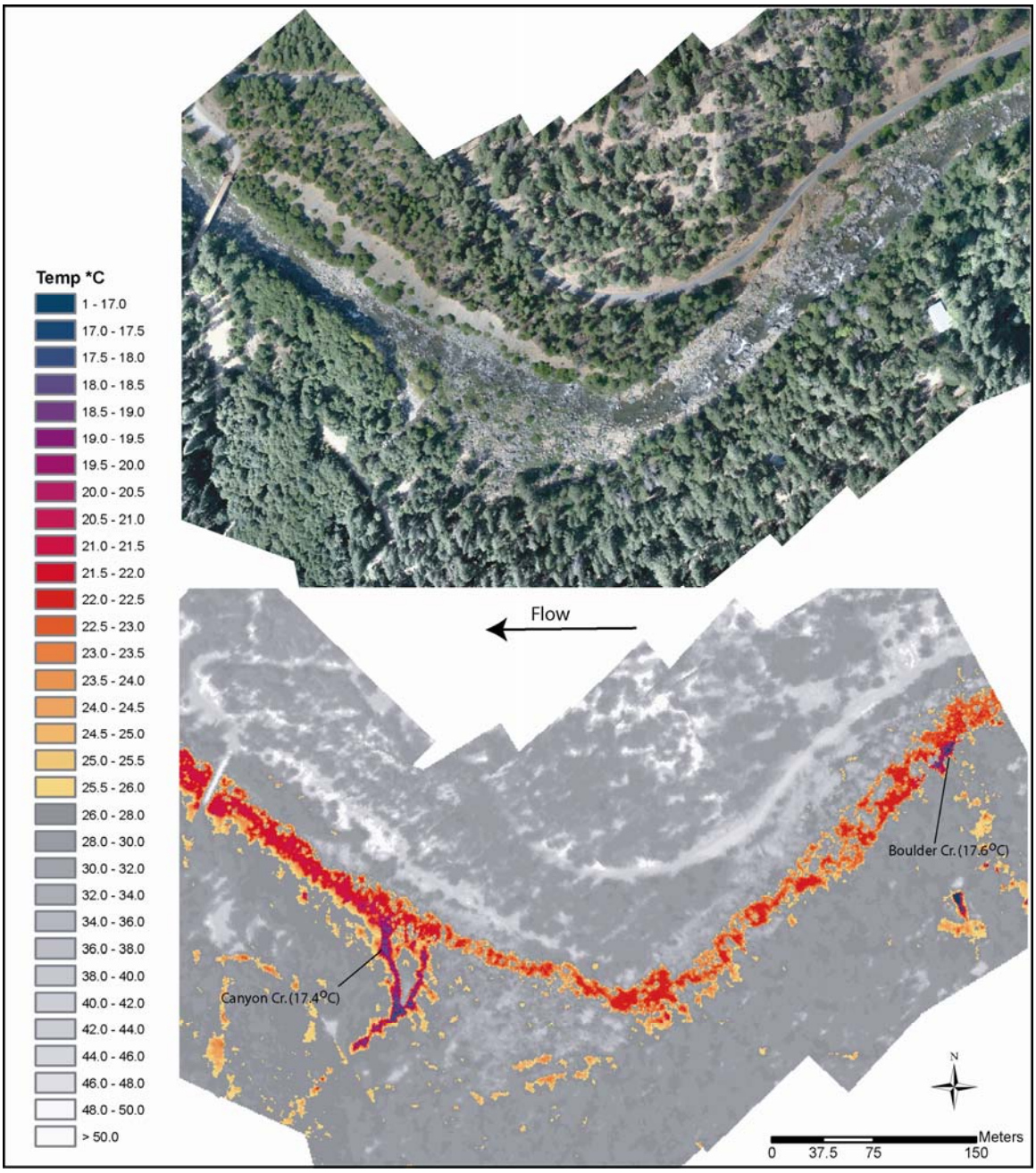

Scott 8 – The TIR (bottom) and true color (top) image shows the confluence of the Scott River and Boulder and Canyon Creeks at river miles 14.7 and 15.9. Both tributaries were cooling sources to the Scott River.

Temperature Patterns 2003 versus 2006

An airborne TIR survey of the Scott River was conducted by Watershed Sciences for researchers at the University of California at Davis and the California North Coast Regional Water Quality Control Board (NCRWQCB) during the summer of 2003. A comparison of the longitudinal temperature profiles from this survey (2006) and the 2003 survey are provided in Figure 7. The profiles were measured using the same general methodology, but with two different make/model thermal sensors. The comparison provides additional insights into the spatial temperature patterns in the Scott River and also how these patterns may have changed with respect to flow conditions and management changes between the two dates.

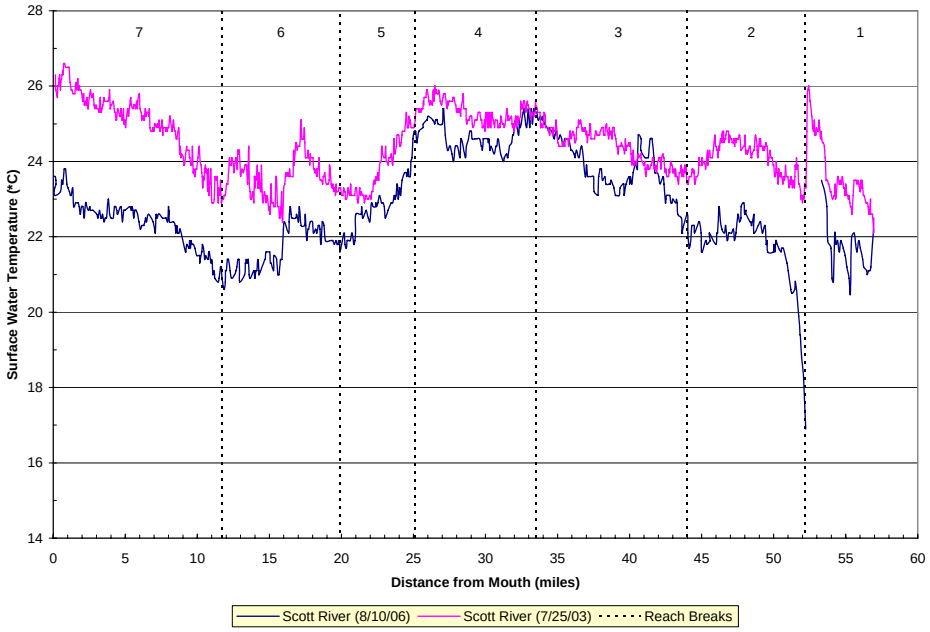

Figure 7 – A comparison of median surface water temperatures in the Scott River measured on August 10, 2006 and July 25, 2003. The temperatures were derived from airborne TIR imagery using the same general methodology.

While the absolute temperatures were generally cooler in 2006, the comparison shows very similar spatial temperature patterns at the reach and basin scale. In some cases, the local temperature patterns within a reach are different. Further analysis of the profiles should consider flow differences between the two dates in addition to changes in management practices, riparian conditions, and other factors that influence water temperatures. The flow levels and average afternoon temperatures for the two survey dates are listed in Table 7.

Table 7 – Flow conditions measured at Fort Jones Station (SFJ, Station 41).

Date	Average Flow	Avg. Air Temp.
July 25, 2003	87 cfs	30.6°C
August 10, 2006	55 cfs	29.9°C

A segmentation of the profile into seven distinct reaches is shown on Figure 7. This segmentation is based entirely on visual inspection of the spatial temperature patterns and considers general trends (i.e. warming, cooling, or variable) at the reach scale. It is recognized that other segmentations are possible depending on spatial scale and evaluation criteria. The following provides a brief comparison of the 2003 and 2006 profiles for each reach.

Reach 1: Local spatial variability observed through the mine tailings. Both the 03 and 06 profiles show sub-surface upwelling at river mile 52.2 and very similar thermal response through this reach.

Reach 2: Both profiles show longitudinal heating downstream of mile 52.2 followed by a slight cooling trend between river mile 47.9 and 44.2. The 2006 profile shows more dramatic heating downstream of mile 52.2 and a higher degree of local spatial temperature variability. These differences may be due to differences in flow conditions between the two dates.

Reach 3: A general downstream warming trend was observed in both profiles for this reach. The 2003 profile shows a 2.0°C water temperature increase while the 2006 profile shows a 3.2°C gain. The 2003 profile did not show the distinct temperature increase and subsequent decrease observed in the 2006 profile between river miles 42.4 and 40.2. This difference may also be due to the differences in flow levels between the two years. However, the true source could not be determined through inspection of the imagery.

Reach 4: The spatial temperature pattern was very similar between the two years with generally warm temperatures and some slight cooling observed between miles 32.6 and 31.6. The sharp increase at mile 27.4 observed in the 2006 profile was not observed in 2003.

Reach 5: Both profiles showed a downstream cooling trend as the river transitions from the broad Scott Valley into the more confined canyon reach. The rate and magnitude of the cooling was similar between the two years.

Reach 6: Both profiles illustrate a slight warming trend between mile 19.9 and the inflow of Boulder and Canyon Creeks. The increase was more dramatic in the 2003 data set. The 2003 profile showed longitudinal heating downstream of river 15.8 that was not measured in the 2006 survey. This was one of the more significant differences in the two profiles.

Reach 7: A consistent longitudinal heating rate was observed in the lower 11.7 miles in both 2003 and 2006.

Shackleford Creek

Longitudinal Profile

Median channel temperatures were plotted versus river mile for Shackleford Creek from its mouth upstream to river mile 9.0 (Figure 8). Tributaries and springs were also sampled during the analysis and illustrated on the longitudinal profile. The tributary locations and temperatures are summarized in Table 8.

Figure 8 – Median channel temperatures versus river mile for Shackleford Creek.

Table 8 - Tributaries sampled along Shackleford Creek.

	Image	km	mile	Tributary °C	Shackleford Cr. °C	Difference °C
Tributary						
Scott River	t09037	0.10	0.00	23.6	dry	n/a
Mill Creek (RB)	t09140	4.59	2.85	18.7	18.8	-0.1
Seep/Spring						
Seep (RB)	t09078	2.12	1.31	17.6	19.3	-1.7
Seep (LB)	t09084	2.32	1.44	16.5	19.6	-3.1
Spring (LB)	t09124	3.89	2.42	17.4	19.6	-2.2

Observation and Analysis

Shackleford Creek was surveyed upstream its mouth to about river mile 9.0. As mentioned previously, the survey was concluded at this point to avoid any conflicts with fire fighting aircraft operating in the region. Inspection of the imagery at the upstream end of the survey showed a fairly narrow stream channel with numerous rapids and falls (Figure 9).

Figure 9 – True color photo showing a falls on Shackleford Creek at mile 7.2.

Radiant water temperatures were relatively cool (~13.0°C) at the upstream end of the survey and warmed progressively downstream reaching ~15.3°C at river mile 6.0. There were several mapped tributaries between miles 6.0 and 9.0 including Big Meadows Creek (mile 7.1). However, the tributaries were either not detected or could not be sampled due the small stream size and canopy closure (*Image Shack1*).

Moving downstream, stream temperatures remained relatively constant (~15.5°C) between river mile 6.0 and 5.0 before increasing steadily to a local maximum of 17.9°C at river mile 4.3. The stream channel was dry between river mile 4.2 and the confluence of Mill Creek at river mile 2.9. At the confluence, Mill Creek appeared to contribute all of the surface flow to the lower reaches of Shackleford Creek (*Image Shack2*).

Downstream of the Mill Creek confluence, radiant water temperatures increased to a local maximum of 19.7°C at mile 2.5. A distinct cooling trend was observed between river mile 2.5 and 2.0 with temperatures decreasing to 17.5°C. Two impoundments/ diversions and one apparent spring were detected in this reach (*Image Shack3*). The magnitude of the decrease and the detection of the seep suggest sub-surface upwelling as the source of thermal cooling. In some cases, the earthen impoundments will create hydraulic head that will create sub-surface flow under and around the dam and result in some localized upwelling downstream. However, it is not possible just through inspection of the imagery to determine the origin of these seeps.

Shackleford Creek exhibited downstream warming downstream of river mile 2.0 before the channel went dry again at river mile 0.4. The channel was mostly dry from mile 0.4 to its confluence with the Scott River (*Image Shack5*). A cool water seep was visible on the TIR imagery at the confluence suggesting that some level sub-surface flow follows the channel pathway and is a potential cooling source to the Scott River.

Sample Images

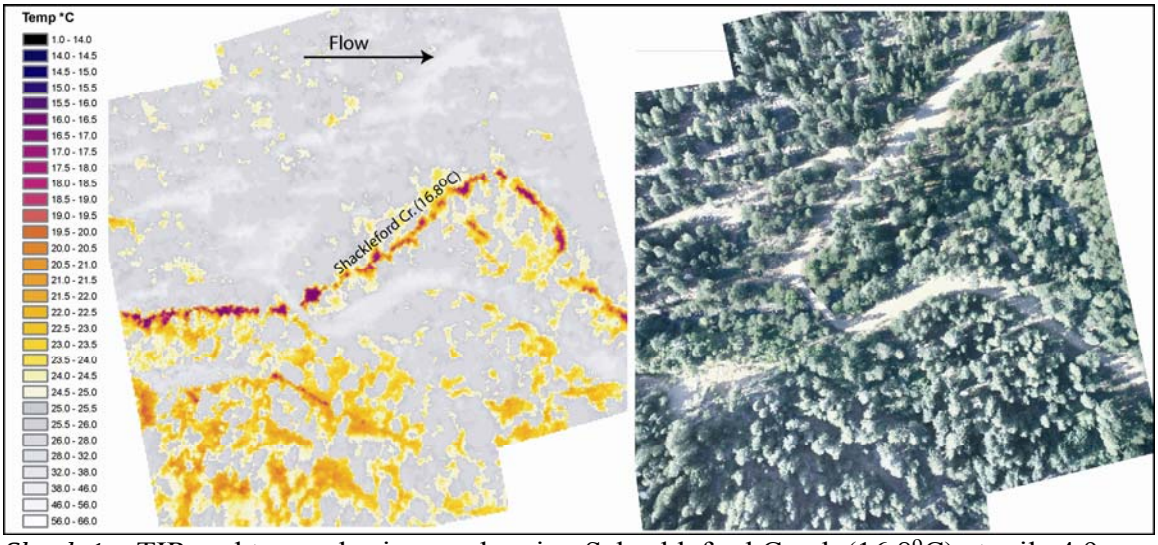

Shack 1 – TIR and true color image showing Schackleford Creek (16.8°C) at mile 4.9. The stream surface was visible through the riparian canopy. However, the stream was more difficult to see as the survey progressed upstream.

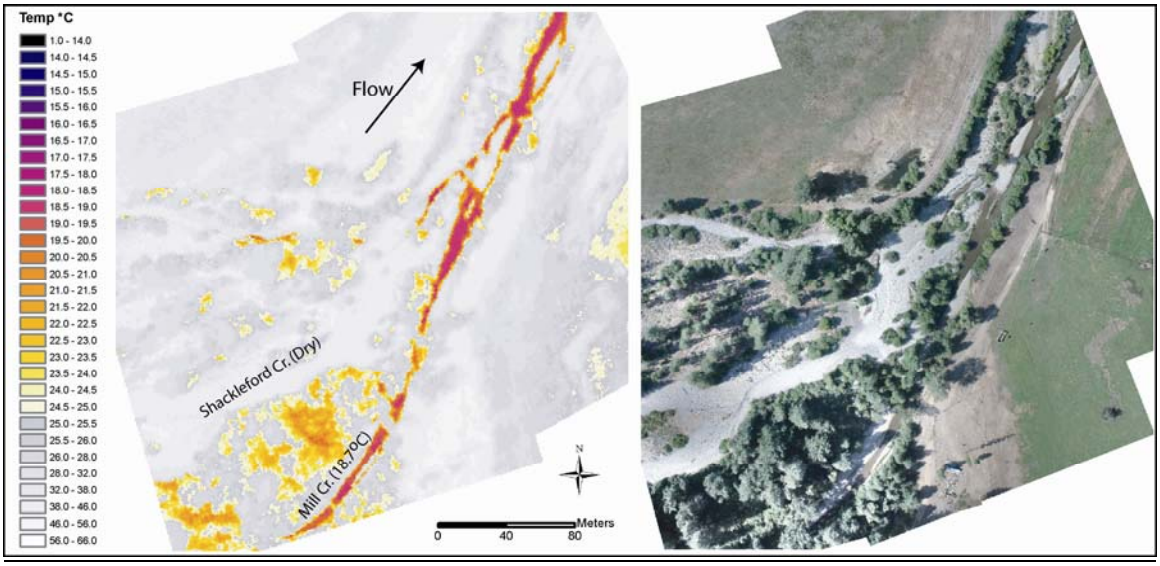

Shack 2 – TIR and true color image showing the confluence of Shackleford Creek and Mill Creek (18.7°C) at mile 2.9. Shackleford Creek was dry upstream of the confluence and Mill Creek supplies all of the surface flow to at this location.

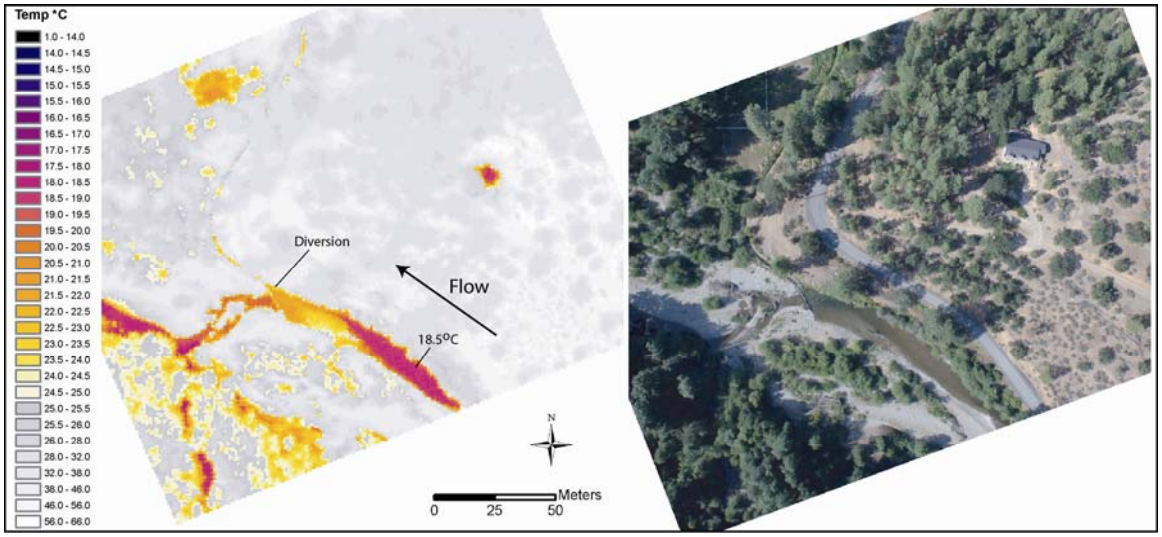

Shack 3 – The TIR (left) and true color (right) image show a diversion in Shackleford Creek (18.4°C) at river mile 2.18. There were several impoundments/diversions detected in Shackleford Creek within this reach. Thermal stratification was evident immediately upstream of the dam.

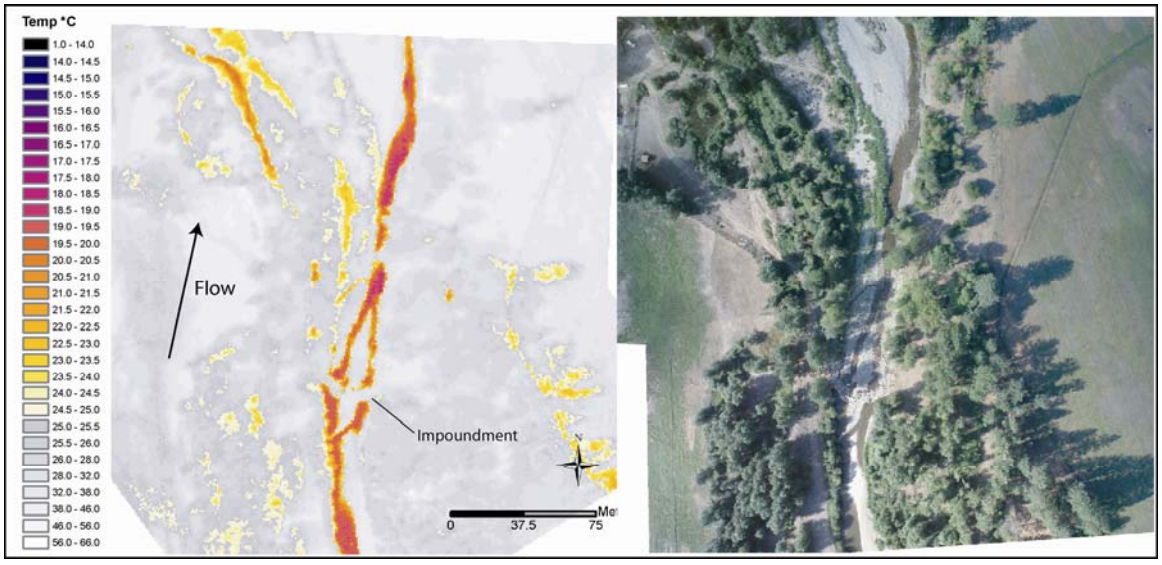

Shack 4 – The TIR (left) and true color (right) image show an impoundment in Shackleford Creek (19.3°C) at river mile 1.3. A cool area detected along the right bank was sampled as a spring/seep (17.6°C). However, due to the size of the stream and the riparian vegetation it was often difficult to determine the source.

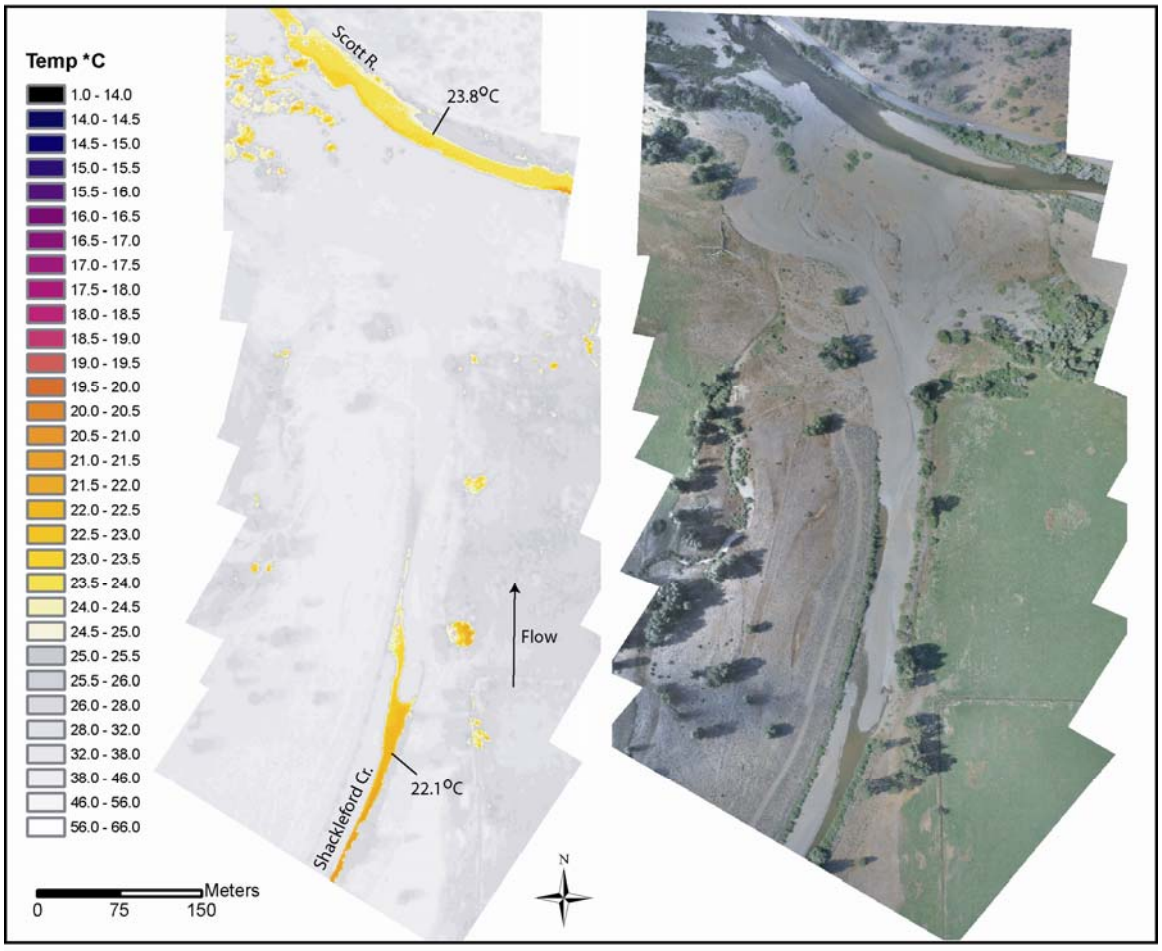

Shack 5 – TIR and true color image showing the confluence of the Scott River (23.8°) and Shackleford Creek. Although the Shackleford Creek channel was dry at the mouth, a small seep was detected at the confluence suggesting some level of sub-surface flow through the channel.

Temperature Patterns 2003 versus 2006

As with the Scott River, an airborne TIR survey was conducted of Shackleford Creek during the summer of 2003. The median temperature data from the 2003 flight were compared to the longitudinal temperature profile from the 2006 flight (Figure 10). The comparison provides insight into how the spatial temperature patterns may have changed during the past three years.

Although the July 26, 2003 profile had overall warmer in-stream temperatures, the longitudinal profiles show very similar spatial temperature patterns. Both profiles showed a warming trend between river mile 9.0 and 6.0 followed by relatively consistent temperatures between mile 6.0 and 5.0. In both years, the profiles showed that water temperatures increased rapidly downstream of mile 4.8 before the channel went completely dry at about mile 4.3.

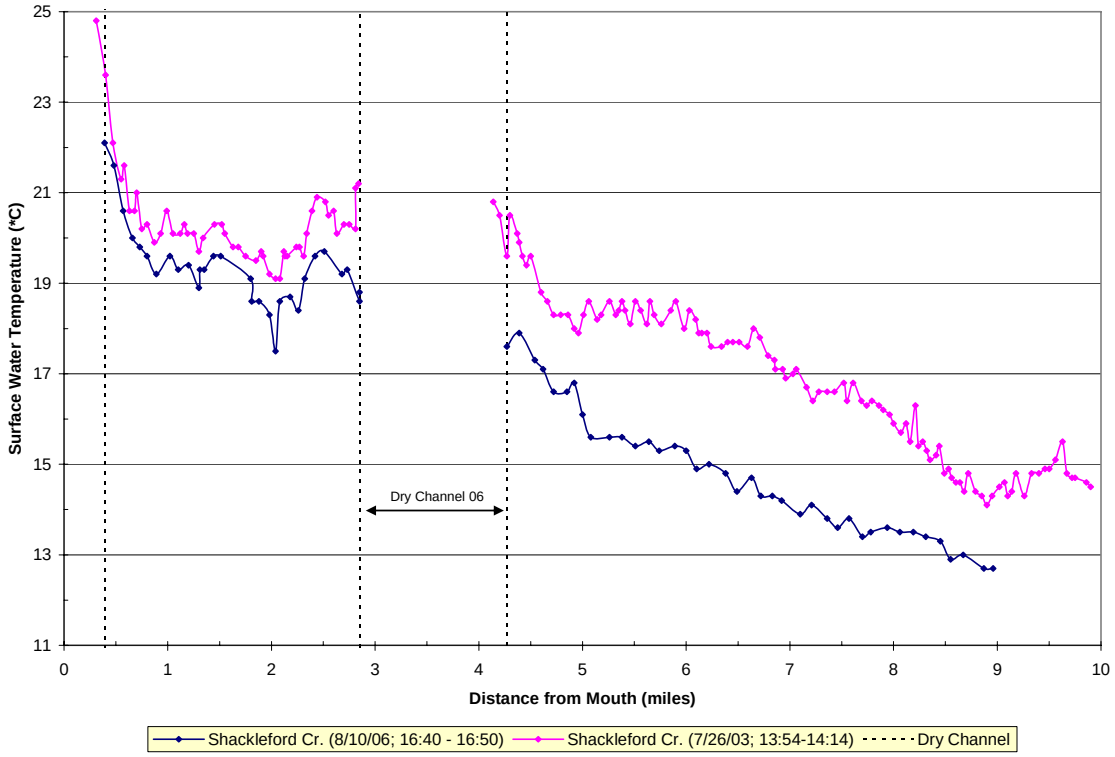

Figure 10 – Comparison of median radiant water temperatures from airborne thermal infrared surveys conducted in 2003 and 2006.

Absolute temperatures were more consistent between the two years downstream of the Mill Creek confluence. In the lower 2.8 miles, the profiles tracked very closely including the detected temperature decrease between river mile 2.5 and 2.0 and the dry channel at the mouth.

The difference in absolute water temperatures is difficult to assess without comparing meteorological and flow conditions between the two years. The 2006 survey, which was also conducted later in the day, had overall cooler temperatures than those observed in the 2003. This was especially obvious upstream of river mile 4.3. The difference suggests either higher flows or overall cooler conditions during 2006.

Summary

Airborne thermal infrared surveys were successfully conducted on Scott River and Shackleford Creek on August 10, 2006. Watershed Sciences deployed in-stream sensors which were used to calibrate and verify the accuracy of the radiant temperatures. The results showed that the radiant temperature accuracies were consistent with previous surveys conducted on other streams in the Western United States.

The TIR imagery and derived products shows how stream temperatures vary spatially along the stream gradient. These data can be used to plan the future field work by identifying optimal locations for temporally continuous data loggers and in-stream flow measurements. The data also identify locations of potential thermal refugia for cold water fish species that hold in the Scott River during the summer months. These data can direct future fish counts and be used to calculate potential carrying capacity. Finally, the data provide baseline inputs for temperature modeling efforts designed to investigate ways to mitigate stream temperatures in the basin.

Deliverables

The data provided with this report are the base data products associated with the airborne TIR image acquisition. These products include: 1) individual un-rectified frames; 2) longitudinal temperature profile; 3) a GIS point layer which provides an index of image locations, the results of temperature sampling, and interpretations made during the analysis; 4) this report.

A follow-on effort (*in progress*) is geo-rectifying the thermal IR imagery to provide a GIS compatible thermal image mosaic of both surveyed streams.

All geo-spatial coverages are saved as: **UTM Zone 10, NAD83, Units = Meters.**

1. Unrectified_Images.
    a. TIR_Frames - Calibrated TIR images in ESRI GRID Format. GRID cell value = radiant temperature * 10. Radiant temperatures are calibrated for the emissive characteristics of water and may not be accurate for terrestrial features. These images retain the native resolution of the sensor.
    b. TC_Frames – Unrectified true color images in jpg format. An index is provided to show the geographic location of the aircraft at the time the image was acquired.
    c. TIR_Psuedo – Unrectified TIR images in "jpg" format. The pixels values have been assigned a color based on temperature ranges. The color index is also provided in this directly. Theses images can be viewed in most image viewing software and directly imported into documents.
2. Longprofile - Excel spreadsheet containing the longitudinal temperature profiles.
3. Survey - Point layers showing image locations, sampled temperatures, and image interpretation.
4. Thermal Mosaics – Geo-rectified thermal imagery in geotiff (.tif) file format. Cell value is radiant temperature * 10.
5. Report – A copy of this report

Contact Information

Russell Faux
111 NW 2nd Street, Unit 1
Corvallis, OR 97330
Office: 541-752-1204
Cell: 541-760-1835